NATIONAL ADVISORY COMMITTEE FOR AERONAUTICS

TECHNICAL MEMORANDUM

No. 1177

WIND-TUNNEL INVESTIGATIONS ON A CHANGED MUSTANG PROFILE WITH NOSE FLAP

FORCE AND PRESSURE-DISTRIBUTION MEASUREMENTS

By W. Krüger

TRANSLATION

"Windkanaluntersuchungen an einem abgeänderten Mustang-Profil mit Nasenklappe. Kraft- und Druckverteilungsmessungen."

Deutsche Luftfahrtforschung, Untersuchungen und Mitteilungen Nr. 3153

Washington

September 1947

NATIONAL ADVISORY COMMITTEE FOR AERONAUTICS

TECHNICAL NOTE NO. 1177

WIND-TUNNEL INVESTIGATIONS ON A CHANGED MUSTANG PROFILE WITH NOSE FLAP

FORCE AND PRESSURE-DISTRIBUTION MEASUREMENTS*

By W. Krüger

Abstract: Measurements are described which were taken in the large wind tunnel of the AVA on a rectangular wing "Mustang 2" with nose flap of a chord of 10 percent. Besides force measurements the results of pressure-distribution measurements are given and compared with those on the same profile "without" nose flap.

Outline:

I. Introduction

II. Model specifications and test arrangement

III. Definitions and evaluation

IV. Test results

V. Summary

VI. References

I. INTRODUCTION

It is known from earlier investigations on wings with nose flap (1 to 3) that the maximum lift can be considerably increased by use of a nose flap as far as profiles are concerned where the point of turbulent separation is located closely behind the profile nose. It has already been pointed out (2) that the $c_{a_{max}}$ increasing effect of the nose flap is the larger the more pointed the profile

*"Windkanaluntersuchungen an einem abgeänderten Mustang-Profil mit Nasenklappe. Kraft- und Druckverteilungsmessungen." Zentrale für wissenschaftliches Berichtswesen der Luftfahrtforschung des Generalluftzeugmeisters (ZWB) Berlin-Adlershof, Untersuchungen und Mitteilungen Nr. 3153, Göttingen, September 22, 1944.

used, that is, the smaller the nose radius index $\frac{\rho/l}{(d/l)^2}$. For instance a measurement on a profile with standard NACA nose radius showed no improvement in $c_{a_{max}}$ by the nose flap (4) whereas $c_{a_{max}}$ of a trapezoid wing with a profile similar to a Mustang profile could be increased by the amount of 0.1 by means of a nose of 5-percent chord ratio (5). For a laminar profile (2) with the nose radius index $\frac{\rho/l}{(d/l)^2} = 0.21$ the largest increase in $c_{a_{max}}$ measured was about 0.7.

For the application of the nose flap for prevention of stall in trapezoid wings a $c_{a_{max}}$-increase of 0.2 to 0.3 would, circumstances permitting, be sufficient because here the point is only to increase slightly the local $c_{a_{max}}$ and $\alpha\left(c_{a_{max}}\right)$ in the endangered part of the wing.

The firm Blohm and Voss Flugzeugbau suggested an investigation on a Mustang profile to determine whether it is possible to obtain such improvements necessary for the prevention of stall by means of a nose flap. The present report contains the results of this test. The measurement could be extended so that also pressure-distribution measurements over nose flap chord and profile chord were carried out. These measurements give information about the changes caused by the flap in the form of the pressure distribution and about the loads for the flap which are to be expected.

II. MODEL SPECIFICATIONS AND TEST ARRANGEMENT

The measurements were carried out in the large wind tunnel of the AVA (K VI), nozzle 5×4.5 meters (elliptic cross section $F_o = 17.6\ m^2$). For the test a wing was at disposal which had been investigated before with and without rear split flap (6). It had then been designated "Mustang 2".

The following specifications concern its form and magnitude:

Span	$b' = 3.0$ m (measured without wing tips)
Maximum span	$b = 3.083$ m (with wing tips)
Chord	$l = 0.6$ m
Wing contour	Rectangular
Wing area of reference	$F = 1.846$ m^2 (measured with wing tips)
Aspect ratio	$\Lambda = \frac{b^2}{F} = 5.14$

The profile Mustang 2 is distinguished from the "Mustang" original profile mainly by a differently formed mean camber line which reduces the diving moment. The basic trains of thoughts with respect to the design of this profile were thoroughly discussed in the report already mentioned on the first measurements (6).

The form of the profile can be seen in figure 1. The essential profile data are given here once more and are compared with Mustang original:

	Mustang 2	Mustang original
Thickness ratio (d/l)	0.136	0.136
Camber ratio (f/l)	.020	.016
Percent thickness $\left(x_d/l\right)$	.390	.390
Percent camber $\left(x_f/l\right)$	.25	.50
Nose radius index $\left(\frac{\rho/l}{(d/l)^2}\right)$	.625	.577
Trailing edge angle (τ)	7.6°	5°

The wing tips were designed in the form which had proved favorable according to investigations of the AVA (7). (From the profile nose to the maximum thickness circular arc, from there to the trailing-edge elliptic arc with maximum profile thickness as major axis of the ellipse.)

The pressure-distribution test section was as usual at a distance of $0.2\ m = 0.133\ \frac{b'}{2}$ from the symmetry plane of the wing in order to avoid disturbing influences of the moment arm.

The split flap used had a chord of $0.2l$ and was deflected by 60° with respect to the profile tangent at $x/l = 0.8$. No measurement was made of the pressure distribution on the split flap since this distribution is practically independent of the profile form and could, therefore, reliably be supplemented by means of existing measurements taken on other profiles.

Nose flaps of a chord ratio $l_N/l = 0.05$ and 0.10 were investigated. The nose flap angle τ_N and the curvature δ at the leading edge of the nose flap could be changed arbitrarily in order to find the optimum condition.

The investigations were limited to measurement of lift, drag, and longitudinal moment for various wing conditions and to measurement of the pressure distribution.

III. DEFINITIONS AND EVALUATION

The designations can be seen in figure 1. The sign and the definitions of the force and moment coefficients correspond to the form DIN L 100. All coefficients are referred to the area (including the wing tips) or to the chord of the smooth profile. The axis of reference for the longitudinal moment is the cross axis lying at $l/4$. To the test results, corrections were applied to obtain results for the infinite extent of the fluid and infinite aspect ratio in the customary manner. The evaluation of the pressure-distribution measurement gave the connection between normal force and angle of attack for the case of plane flow ("plane" in good approximation!). The effective angle of attack at the location of the pressure test section was calculated from the difference between the geometrical and the induced angle of attack α_i at this point (compare (6)). The pressure-distribution measurement simultaneously yields the normal-force coefficient of the nose flap. This coefficient is referred to the chord of the nose flap l_N.

IV. TEST RESULTS

The Reynolds number for the force measurements was $Re = 2.14 \times 10^6$, for the pressure-distribution measurements $Re = 1.3 \times 10^6$. The results are represented in the figures 2 to 10. Following several comments are given:

1. Obtained Effect of the Nose Flap

Figure 2 shows that, for the most favorable nose-flap angle, $c_{a_{max}}$ of the smooth profile can be increased by 0.3 and α_∞, $\left(\text{for } c_{a_{max}}\right)$, by 5° by means of a nose flap of 10-percent chord ratio. The effect is smaller for the wing with split flap. Here the $c_{a_{max}}$-increase amounts for the most favorable case to 0.15. By means of a flap of 5-percent chord ratio the $c_{a_{max}}$ of the smooth profile can be increased no longer; the maximum lift even decreases slightly. According to these results the assumption may seem permissible that it is possible by means of a flap of about 7-percent chord ratio just to reach the $c_{a_{max}}$ of the smooth profile, yet to retain the advantage of the flatness of the $c_{a_{max}}$-curve of the flap of 5-percent chord ratio. Figure 3 represents the dependence of the $\Delta c_{a_{max}}$ obtained by the nose flap on the nose-flap angle. The optimum angle is smaller for the wing with rear split flap than without split flap.

In figure 7 the courses of the curves $c_n(\alpha)$ resulting from force and pressure-distribution measurements are compared. The rather bad agreement is probably caused by the fact that the calculation for determining the induced angle of attack at the location of the section of pressure measurement was performed in first approximation with the mean $dc_a/d\alpha_\infty$ of the smooth profile whereas, more accurately, the $dc_a/d\alpha_\infty$ of the nose-flap profile for the angle of attack considered at the time ought to be inserted.

2. Pressure Distribution for Deflected Nose Flap

Figures 4 and 5 show the pressure distribution for various angles of attack for the nose-flap wing without and with split flap. A comparison of the pressure distribution without and with nose flap is made in figure 6. One can recognize the reduction of

the negative pressure peak at the profile nose caused by the nose flap for maximum lift of the profile. Figure 8 makes these relations even more clear. For instance for the wing with split flap, without nose flap, the maximum negative pressure for $c_{n_{max}} = 2.45$ reaches the value $p/q = -15.4$. For larger $c_{n_{max}}$ (2.65) the maximum negative pressure is reduced to $p/q = -7.9$ by the nose flap. Thus the pressure increase in the flow immediately behind the profile nose is considerably reduced by the nose flap. The reason for this slight degree of improvement of the maximum lift coefficient obtainable probably is that for this profile the point of turbulent separation travels with increasing angle of attack from the trailing edge to the front whereas for profiles with very pointed nose, if the critical angle of attack is exceeded the turbulent separation takes place shortly behind the steep pressure increase behind the profile nose. A reduction of the negative pressure peak at the nose by a nose flap must, therefore, have a much more favorable effect with respect to $c_{a_{max}}$ for pointed profiles. Since the nose-radius index of the Mustang original profile is by about 8 percent smaller than the one of the investigated changed profile, it is to be expected that the effectiveness of the nose flap will be somewhat greater for the original profile.

3. Effect of the Curvature of the Leading Edge of the Nose Flap

Systematic investigations on a laminar wing with nose flap (2) had brought the result that the lift-increasing effect of the flap can be improved within certain limits by increased curvature (δ) of the leading edge of the flap. On the other hand, no improvement could be obtained, in the present test, by increase of the rounding off from $\delta/l_N = 0.167$ to $\delta/l_N = 0.334$. The relating test results are not indicated in the curves.

4. Effect of Disturbances at the Flap-Wing Transition

In the measurements a small groove was located at the transition from the nose flap to the wing, the depth and width of which was about 0.5 percent of the wing chord. A comparative measurement for which the transition was smoothed out with clay did not yield any noticeable improvement of the maximum lift. The influence of discontinuities of this order of magnitude is, therefore, negligible for this profile.

However, if, due to leaking at the transition, air can flow through the slot from the flap pressure side to the suction side,

the $\Delta c_{a_{max}}$ of the nose flap will be reduced to about 70 to 50 percent for the present case. In the measurement represented in the figures, clay was made to cover the groove between nose flap and wing so that no air could flow through.

5. Load of the Nose Flap

The pressure distribution along the nose-flap chord for the most favorable flap angle is plotted in figures 9 and 10 for the nose-flap wing with and without split flap. For the larger angles of attack of the wing the entire pressure side of the nose flap is loaded with about the full stagnation pressure. The normal-force coefficient of the flap $c_{n_K} = \frac{N_N}{qbl_N}$ reaches a maximum value of about 3.7.

V. SUMMARY

The effect of a nose flap was investigated by force and pressure-distribution measurements on a profile very similar to the Mustang profile. The purpose of the test was to determine, whether an increase of the $c_{a_{max}}$ and $\alpha c_{a_{max}}$ on this profile can be obtained by means of nose flaps which would be sufficient to improve the stalling behaviour of trapezoid wings.

RESULTS

1. The $c_{a_{max}}$ of the smooth profile was 1.13 $\left(Re = 2.14 \times 10^6\right)$. By a nose flap of 10-percent chord ratio it was increased to 1.43. $\left(\Delta c_{a_{max_N}} = 0.3\right)$. α_∞ for $c_{a_{max}}$ was thereby increased by 5°. The flap appears suitable for use for prevention of stall.

2. The $c_{a_{max}}$ of the split-flap wing $\left(l_K/l = 0.2, \quad \eta_K = 60°\right)$ was increased by the same nose flap by only $\Delta c_a = 0.15$.

3. The minimum nose-flap chord ratio l_N/l necessary is according to the measurements about 7 percent. For smaller chord

ratio $c_{a_{max}}$ decreases as compared with the $c_{a_{max}}$ of the smooth wing; the higher part of the $c_{a_{max}}$-curve, however, is here also very flat.

4. The maximum negative pressure occurring at the profile nose for maximum lift is very considerably reduced by the nose flap.

5. The normal-force coefficient of the flap referred to stagnation pressure and nose-flap area reaches the maximum value $c_{n_N} = 3.7$.

6. The transition from the nose flap to the wing must be airtight. A weak flow through the slot from the pressure side of the flap to the suction side would reduce the effect considerably.

7. For the "Mustang" original profile a slight improvement of the nose-flap effect is to be expected because its nose radius index $\frac{\rho/l}{(d/l)^2}$ is by about 8 percent smaller than the one of the investigated changed Mustang profile.

Translation by Mary L. Mahler
National Advisory Committee
for Aeronautics

VI. REFERENCES

1. Krüger, W.: Ueber eine neue Möglichkeit der Steigerung des Höchstauftriebes von Hochgeschwindigkeitsprofilen. UM Nr. 3049.

2. Krüger, W.: Systematic Wind-Tunnel Measurements on a Laminar Wing with Nose Flap. NACA TM No. 1119, 1947.

3. Riegels, F.: Russische Laminarprofile. 3.Teil: Messungen am Profil 2315 Bis mit AVA-Nasenklappe. UM Nr. 3067.

4. Ehrhardt: Windkanaluntersuchungen mit einer Nasenklappe. Windkanalbericht 7/44 Messerschmitt A.G.

5. Mestern: BV 155 – Flügel mit AVA – Nasenklappe, Bericht WK 44 Blohm und Voss Flugzeugbau.

6. Walz, A.: Messungen an zwei 13,6 o/o dicken Profilen mit kleinem Hinterkantenwinkel im grossen AVA – Kanal. UM Nr. 3092.

7. Regenscheit, B.: Untersuchungen über den Einfluss der Randkappenform auf die Tragflugelmessergebnisse. Techn.Berichte Bd. 11 (1944) Nr. 5.

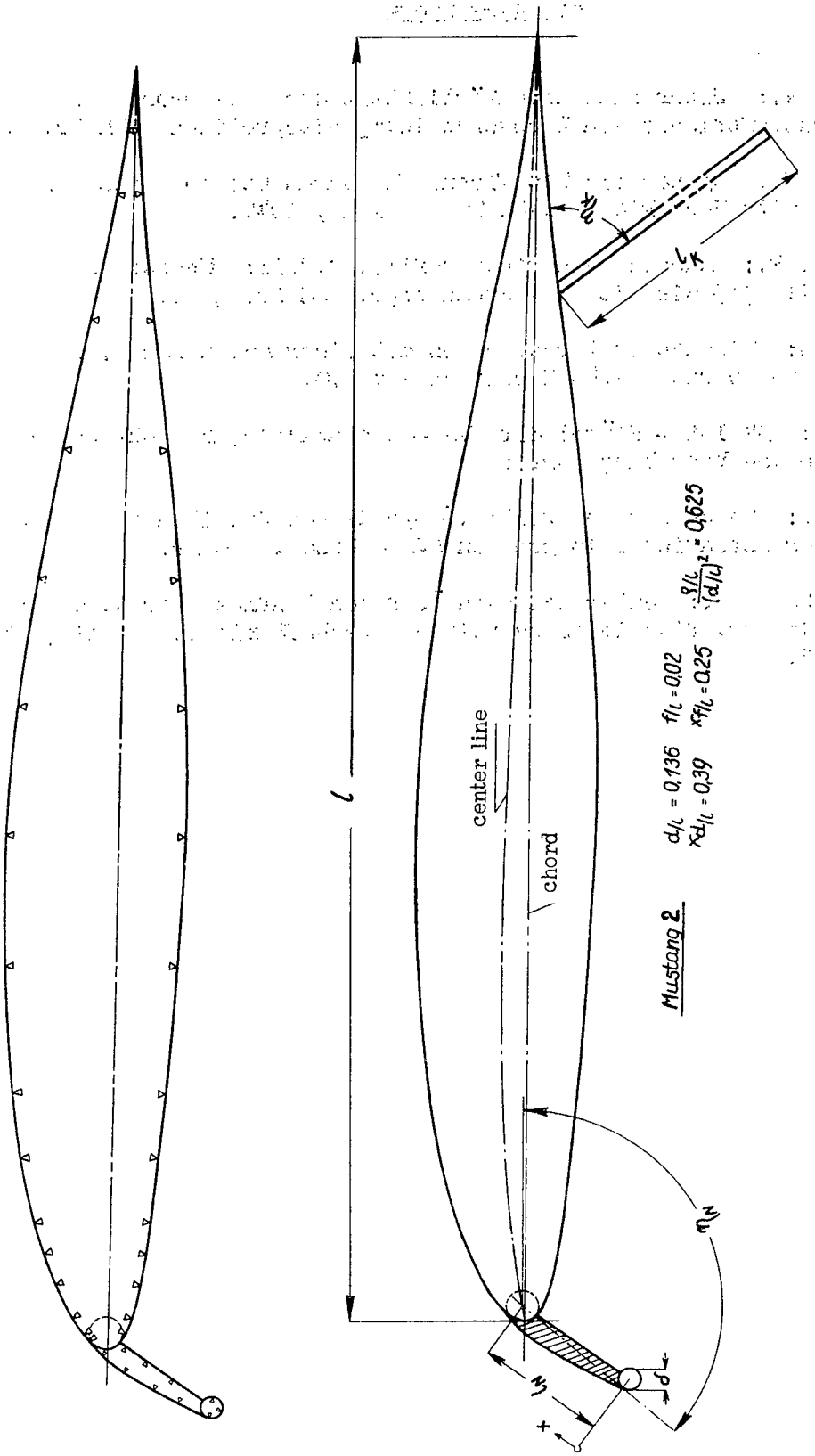

Figure 1.- The investigated profile.

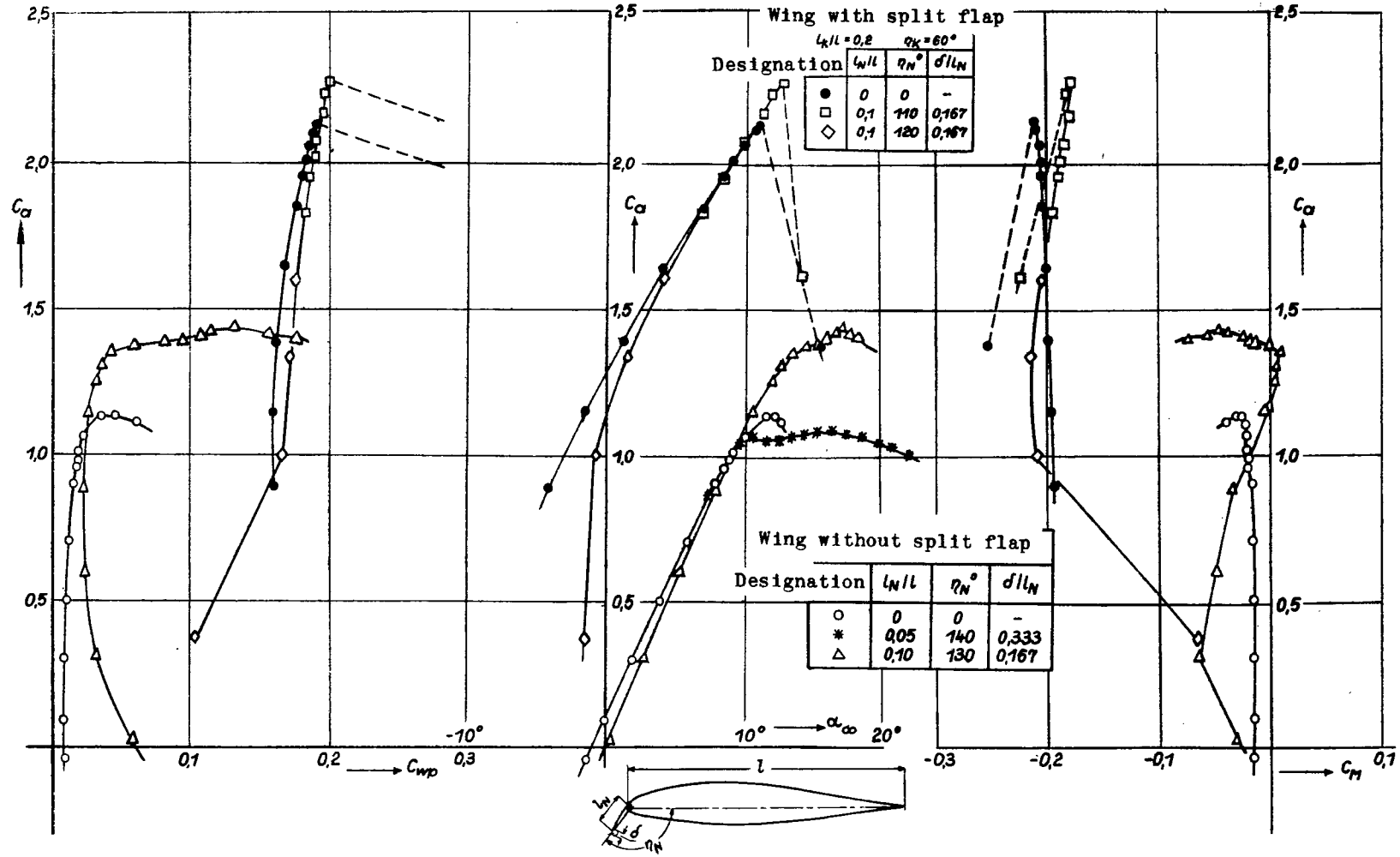

Figure 2.- Influence of the nose flap on the aerodynamic coefficients of the profile with and without split flap. Valid for the most favourable nose flap angle η_N. The nose flap camber is selected so that it coincides for the retracted condition with the pressure side contour of the smooth profile.

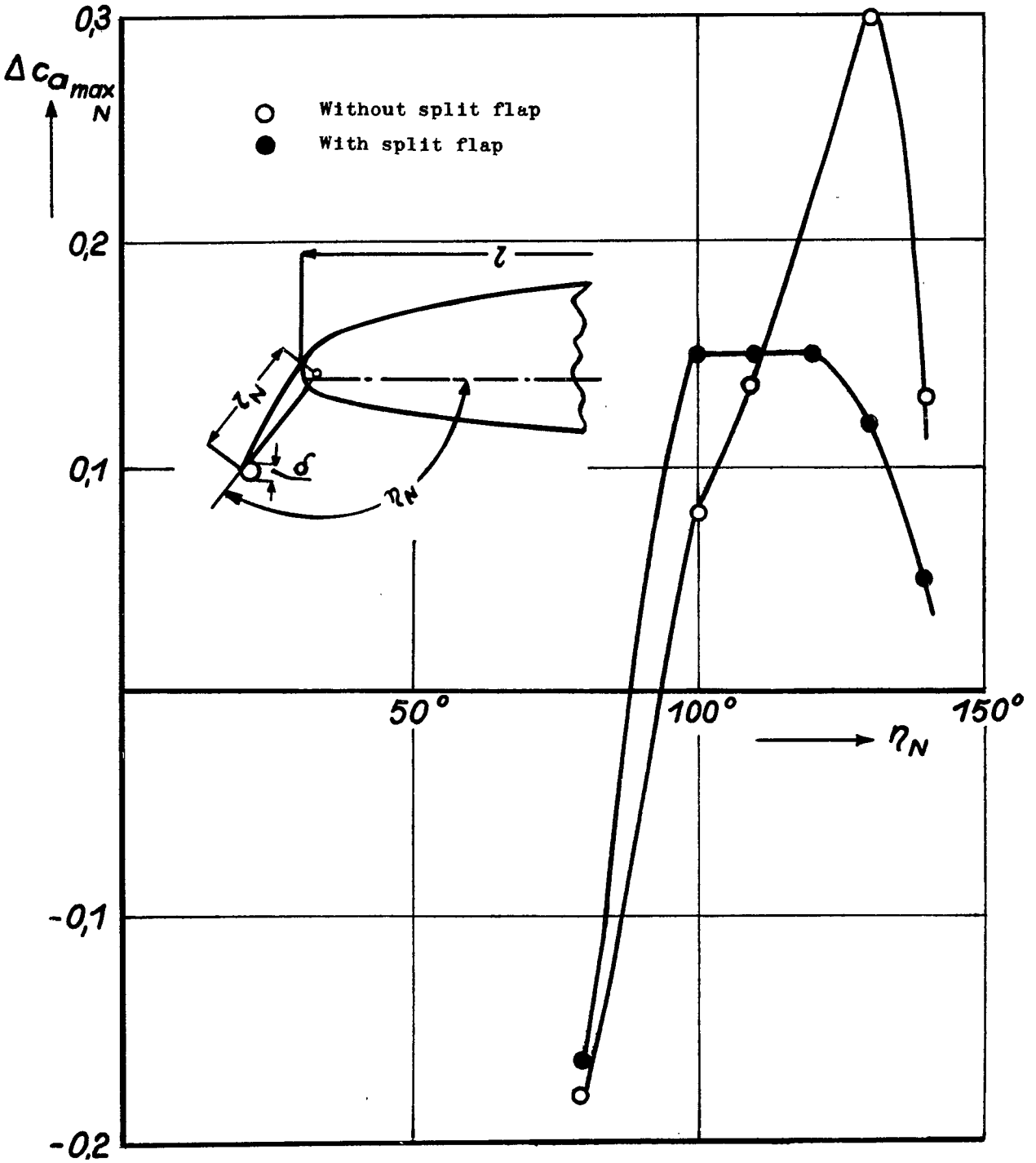

Figure 3.- Increase of the maximum lift coefficient by the effect of the nose flap as a function of the angle of extension η_N. Valid for: $l_N/l = 0.1$, $\delta/l_N = 0.167$.

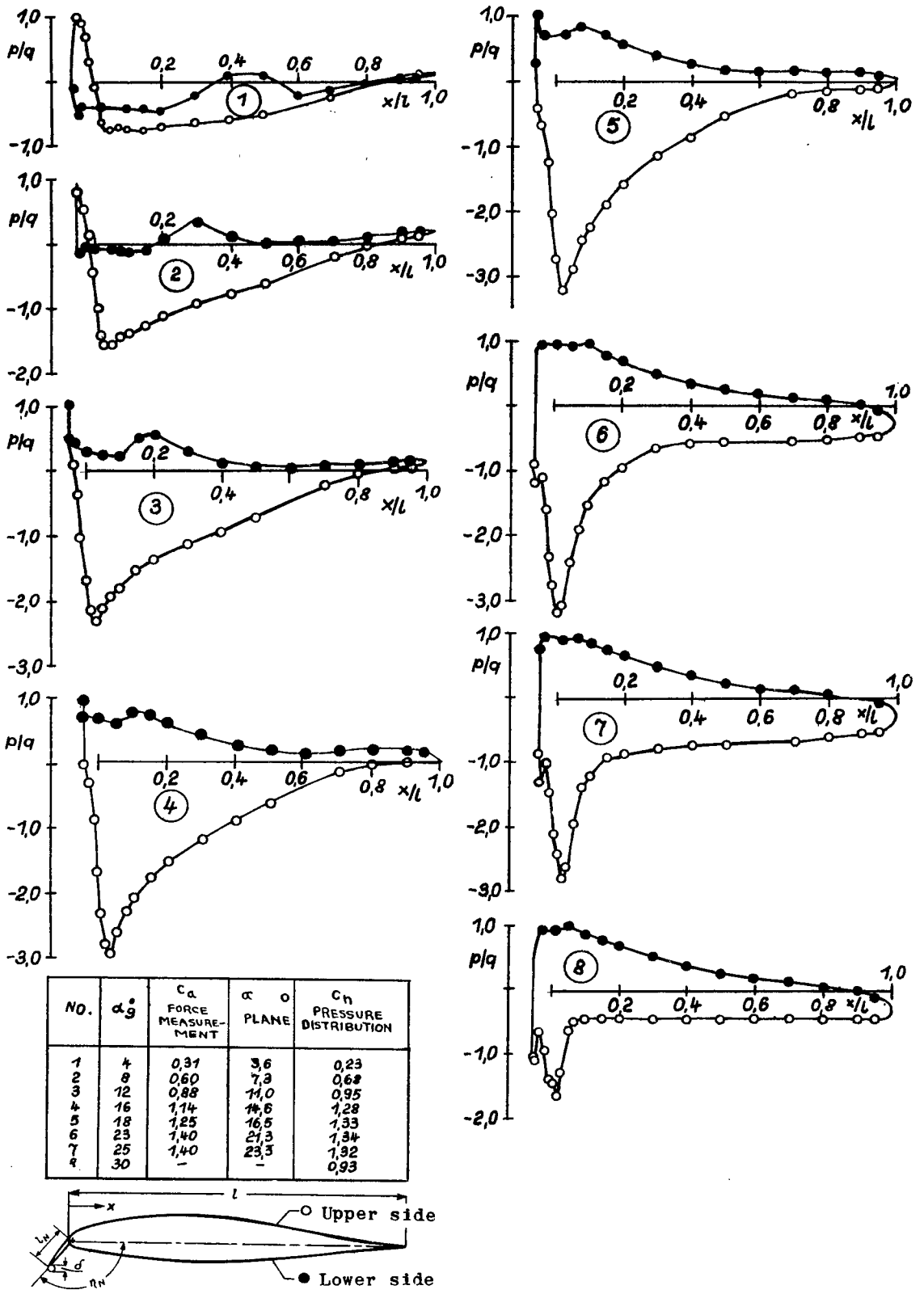

No.	α_g°	c_a force measurement	α_o plane	c_h pressure distribution
1	4	0,31	3,6	0,23
2	8	0,60	7,3	0,62
3	12	0,88	11,0	0,95
4	16	1,14	14,6	1,28
5	18	1,25	16,5	1,33
6	23	1,40	21,3	1,34
7	25	1,40	23,3	1,92
8	30	–	–	0,93

Figure 4.- Pressure distribution along the profile chord for the wing with nose flap. $l_N/l = 0.1$; $\delta/l_N = 0.167$; $\eta_N = \eta_{Nopt} = 130^\circ$.

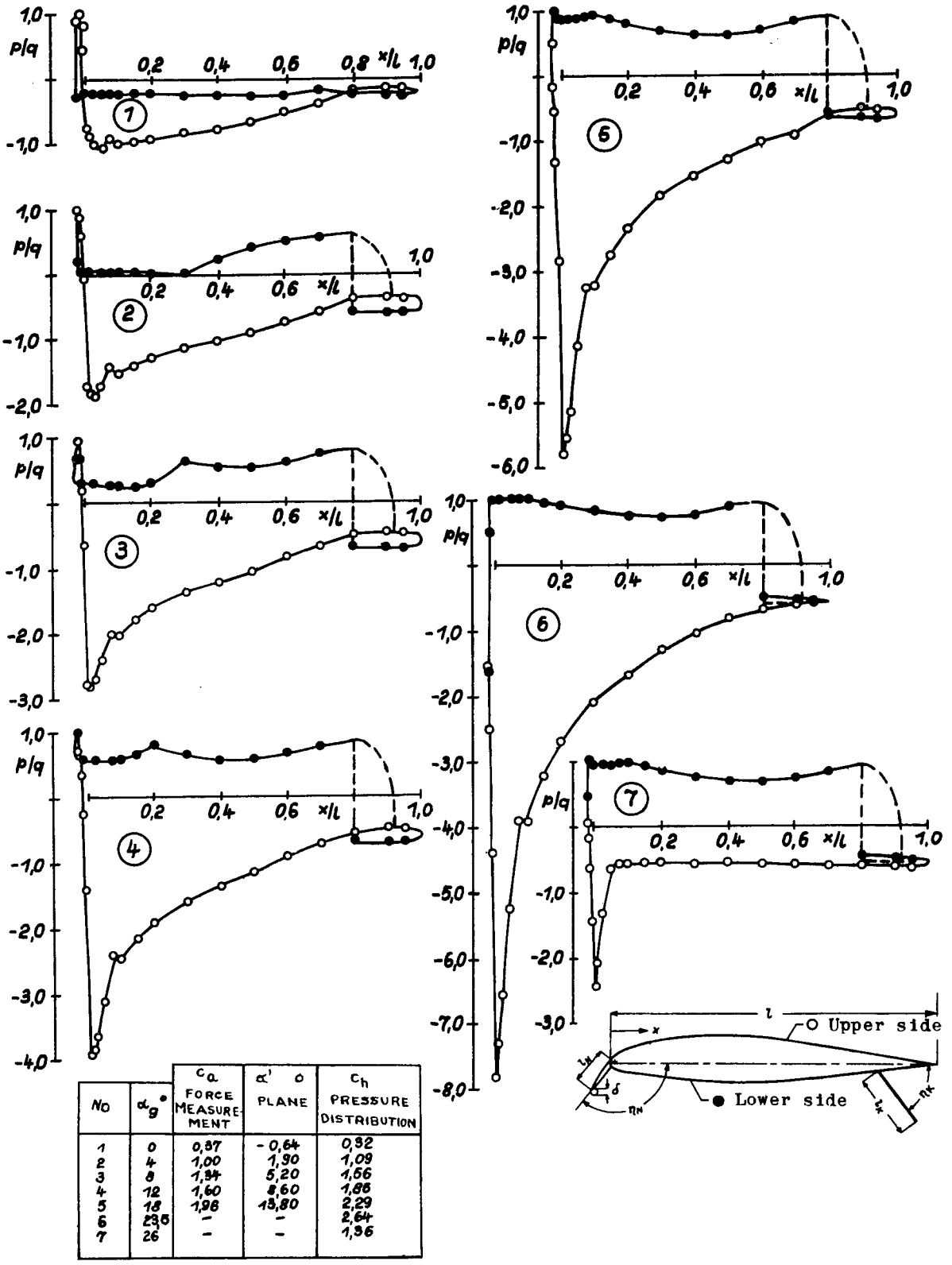

No	α_g °	c_a FORCE MEASUREMENT	α' ° PLANE	c_h PRESSURE DISTRIBUTION
1	0	0,37	- 0,64	0,92
2	4	1,00	1,90	1,09
3	8	1,94	5,20	1,56
4	12	1,60	8,60	1,86
5	18	1,98	13,80	2,29
6	23,5	–	–	2,64
7	26	–	–	1,96

Figure 5.- Pressure distribution along the profile chord for the wing with split and nose flap. $l_K/l = 0.2$; $l_N/l = 0.1$; $\eta_K = 60^\circ$; $\eta_N = \eta_{Nopt} = 110^\circ$; $\delta/l_N = 0.167$.

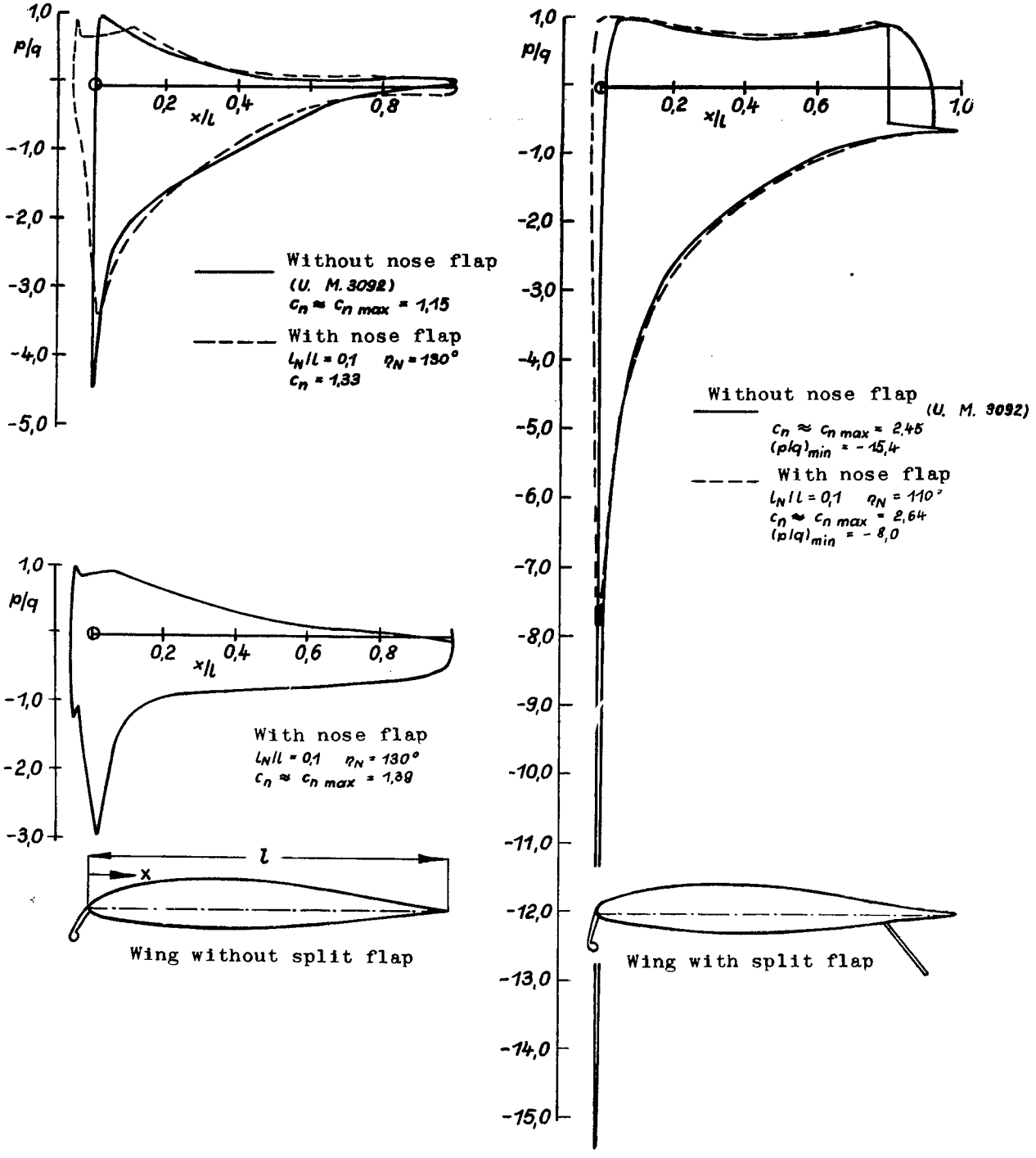

Figure 6.- Variation of the pressure distribution along the profile chord at $c_{a_{max}}$ by the nose flap. The pressure distributions "without nose flap" are taken from the report U. M. No. 3092.

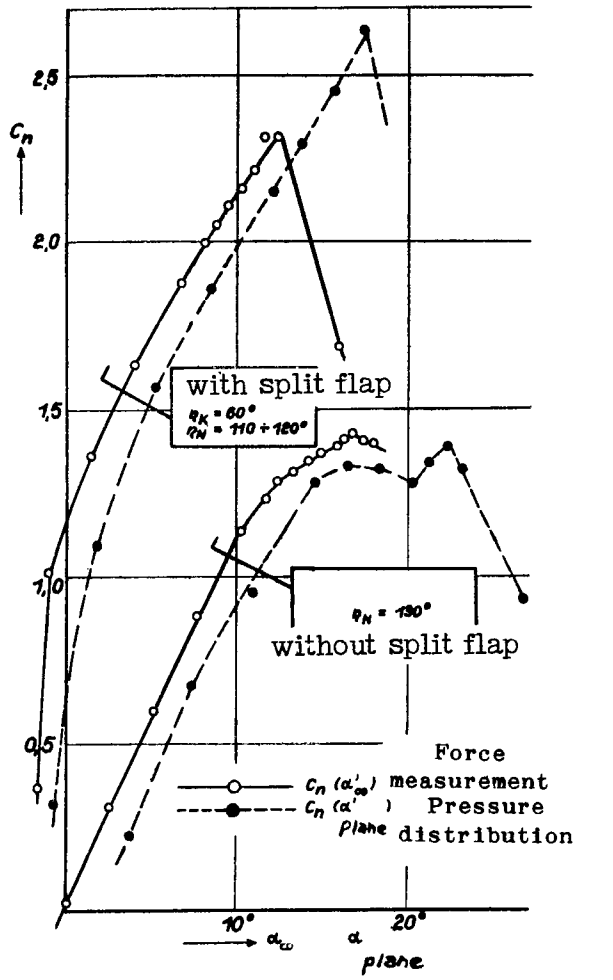

Figure 7.- Normal force coefficient as a function of the angle of attack. Wing with nose flap l_N/l = 0.1, δ/l_N = 0.167. Comparison between force and pressure distribution measurement.

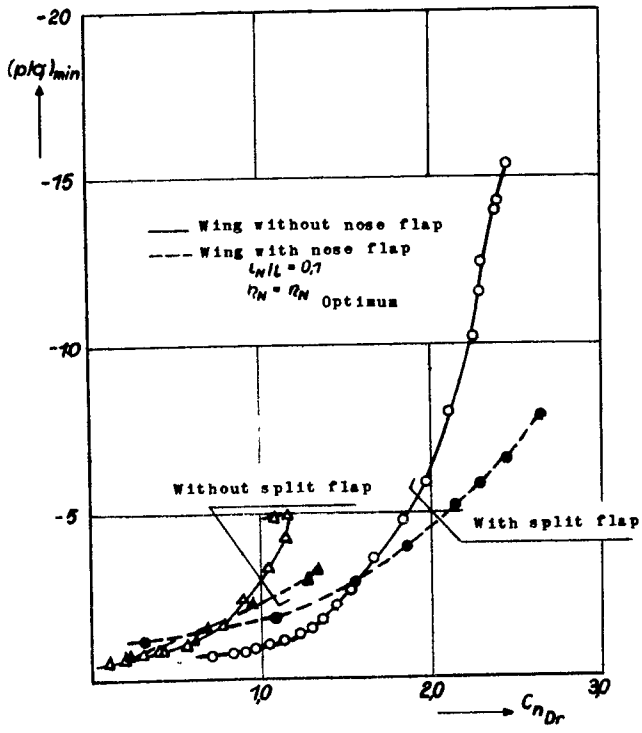

Figure 8.- Negative pressure peak at the nose of the profile as a function of the normal force coefficient (from pressure distribution measurement).

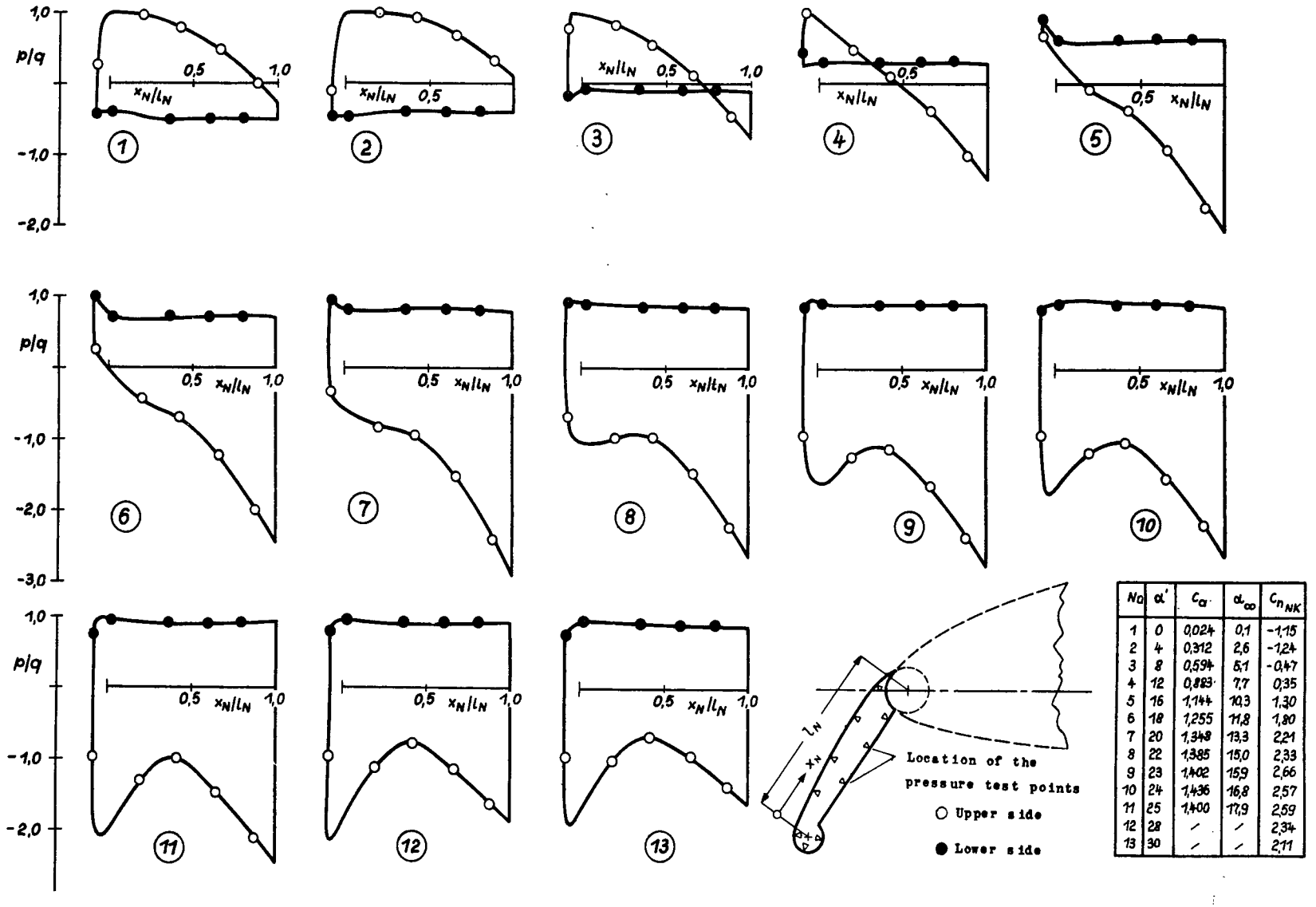

No	α'	c_a	α_{a0}	$c_{n_{NK}}$
1	0	0,024	0,1	-1,15
2	4	0,312	2,6	-1,24
3	8	0,594	5,1	-0,47
4	12	0,883	7,7	0,35
5	16	1,144	10,3	1,30
6	18	1,255	11,8	1,80
7	20	1,348	13,3	2,21
8	22	1,385	15,0	2,33
9	23	1,402	15,9	2,66
10	24	1,436	16,8	2,57
11	25	1,400	17,9	2,59
12	28	/	/	2,34
13	30	/	/	2,11

Figure 9.- Pressure distribution along the nose flap chord. Profile without split flap. $l_N/l = 0.1$; $\delta/l_N = 0.167$; $\eta_N = \eta_{Nopt} = 130^\circ$.

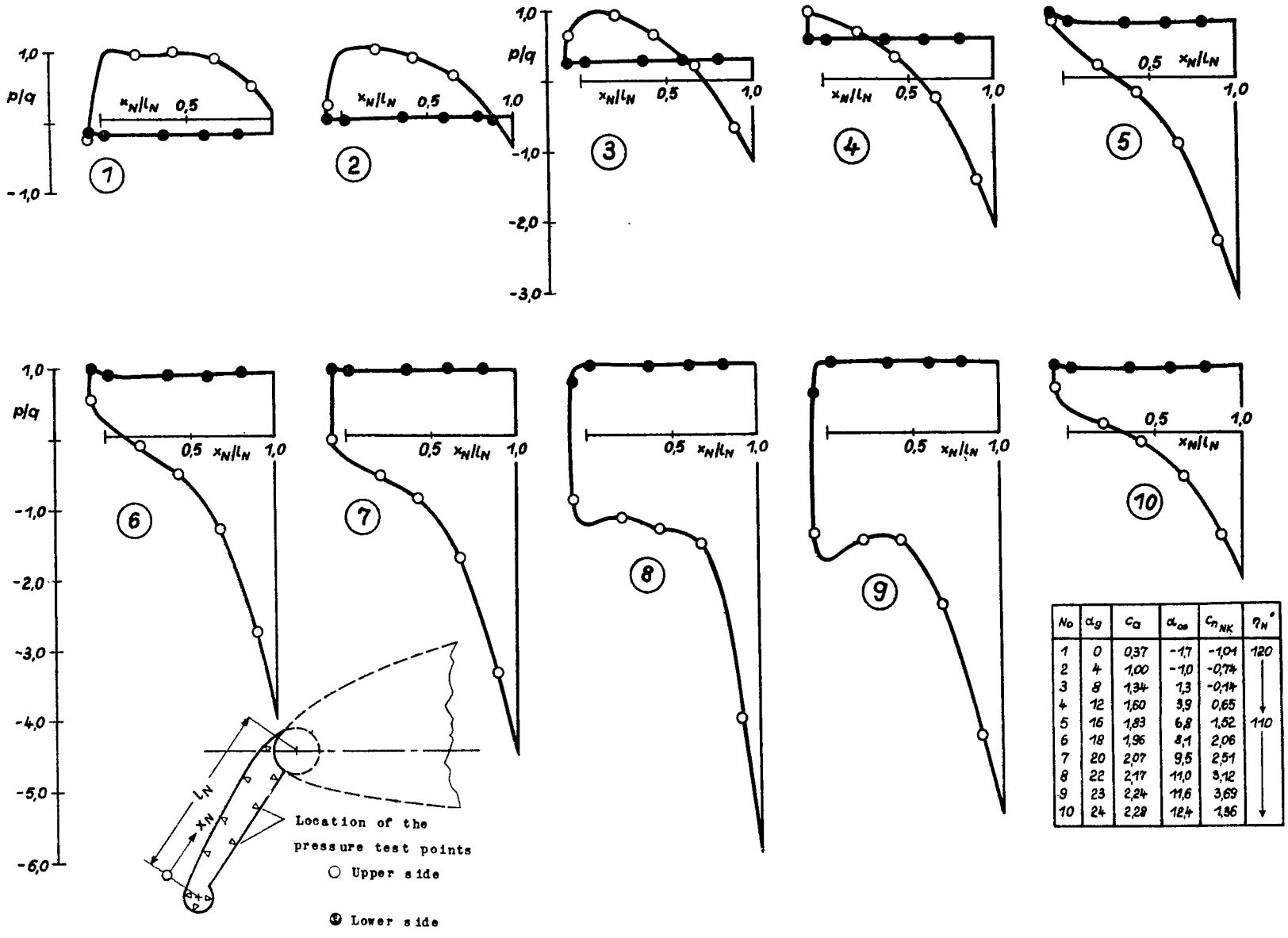

No	α_g	c_a	$\alpha_{a=0}$	$c_{n_{NK}}$	η_N
1	0	0,37	-1,7	-1,01	120
2	4	1,00	-1,0	-0,74	
3	8	1,34	1,3	-0,14	
4	12	1,60	3,9	0,65	
5	16	1,83	6,8	1,52	110
6	18	1,96	8,1	2,06	
7	20	2,07	9,5	2,51	
8	22	2,17	11,0	3,12	
9	23	2,24	11,6	3,69	
10	24	2,29	12,4	1,86	

Figure 10.- Pressure distribution along the nose flap chord. Profile with split flap. $l_K/l = 0.2$; $\eta_K = 60^\circ$; $l_N/l = 0.1$; $\eta_N = 120^\circ$ or 110°; $\delta/l_N = 0.167$.